NJC

Accepted Manuscript

This is an *Accepted Manuscript*, which has been through the Royal Society of Chemistry peer review process and has been accepted for publication.

Accepted Manuscripts are published online shortly after acceptance, before technical editing, formatting and proof reading. Using this free service, authors can make their results available to the community, in citable form, before we publish the edited article. We will replace this *Accepted Manuscript* with the edited and formatted *Advance Article* as soon as it is available.

You can find more information about *Accepted Manuscripts* in the Information for Authors.

Please note that technical editing may introduce minor changes to the text and/or graphics, which may alter content. The journal's standard Terms & Conditions and the Ethical guidelines still apply. In no event shall the Royal Society of Chemistry be held responsible for any errors or omissions in this *Accepted Manuscript* or any consequences arising from the use of any information it contains.

ROYAL SOCIETY OF CHEMISTRY

www.rsc.org/njc

Synthesis, controlled release and antibacterial studies of nalidixic acid-zinc hydroxide nitrate nanocomposites

Hafezeh Nabipour[1*], Moayad Hossaini Sadr[1], Nygil Thomas[2]

[1]*Chemistry Department, Faculty of Science, Azarbaijan Shahid Madani University, Tabriz, Iran.*

[2]*Post Graduate and Research Department of Chemistry, Nirmalagiri College, Kannur, Kerala, India, 670701.*

Abstract:

Nalidixic acid (NA) was intercalated in zinc hydroxide nitrate (ZHN) by ion exchange method. The resulted nanocomposite showed a basal spacing of 11.74 Å that corresponds to a pure phase, confirmed by Powder X-ray Diffraction (PXRD) studies. The arrangement of NA in the interlayer of ZHN was in a monolayer form. FTIR spectroscopy study showed that the intercalation took place without any change in the structure of the NA and the thermal analysis results showed that the NA is stabilized in the interlayers by electrostatic interactions. The biocompatible NA-ZHN/chitosan nanocomposites were prepared by coating of NA-ZHN nanocomposite with chitosan and drug release behavior *in vitro* was studied. The antibacterial activities of nanocomposite tested against microorganisms. The results showed that the synthesized nanocomposites have good inhibition against two gram-positive and gram-negative species. NA-ZHN can prevent the growth of harmful bacteria more effectively than the NA drug.

Keywords: Nalidixic acid; Zinc hydroxide nitrate; Nanocomposite; Antibacterial activity

*Corresponding author mail address:ha.nabipour@gmail.com, Tel: +984134327500, Fax: +984134327541

1. Introduction

The brucite-like layered metal hydroxide compounds can be broadly classified into two types based on their structure and chemical compositions [1]. Layered double hydroxides (LDH) ($LDH - M^{2+}_{1-x}M^{3+}_{x}(OH)_2(A^{m-})_{x/m}.nH_2O$) and layered hydroxide salts (LHS) ($LHS - M^{2+}(OH)_{2-x}(A^{m-})_{x/m}.nH_2O$) are layered crystalline materials belong to the layered metal hydroxide family [2]. LDH and LHS have attracted considerable attention due to its technological importance in catalysis, separation technology, nanocomposite materials engineering [3], matrices for immobilization of different metallocomplexes, magnetic material [4,5], controlled release formulation, slow-release fertilizers [6,7], pharmaceutical products [8,9] and polymer reinforcement materials [10,11]. Zinc hydroxide nitrate (ZHN) is a layered hydroxide salt that can be classified into two sub groups [12]. In Type I with the empirical formula $Zn_2(OH)_2(NO_3)_2{\cdot}2H_2O$, Zn^{2+}cation is coordinated octahedrally with six OH groups, and the nitrate anion are present between the hydroxide layers and coordinated to the Zn^{2+}cations [13]and type IIa and IIb: with formula $Zn_5(OH)_8(NO_3)_2{\cdot}2H_2O$, $Zn_5(OH)_8(NO_3)_2$. In both of these, one quarter of the octahedral zinc cations are displaced from the main layer to tetrahedral sites located above and below each empty octahedron. The hydroxide ions are shared with the octahedral sheet occupy the three vertices of the tetrahedron, the apex is occupied by water molecules in type IIa and takes on a $Zn_5(OH)_8(NO_3)_2{\cdot}2H_2O$ structures [14]. However, in Type IIb, nitrate ions occupying the apex and are directly coordinated with the zinc tetrahedron [12]. ZHN has also been used as a drug delivery system for compounds like ellagic acid [15], cetirizine [16], and protocatechuate [17].

Nalidixic acid (1-ethyl-1,4-dihydro-7- methyl-4-oxo-1,8-naphthyridine-3-carboxylic acid), shown in Figure 1,is the first synthetic quinolone antibiotics that introduced in therapy in the 1960s [18]. NA is effective against both Gram-positive and Gram-negative bacteria. It acts as a bacteriostatic in lower concentrations but can be bactericidal at higher concentrations. Markos

Trikeriotis and Demetrios F. Ghanotakis [19] studied intercalation and release profiles of NA in LDH. Zinc, an essential trace element in human body, takes part in the catalytic activity of approximately 100 enzymes and plays a role in immune function, protein synthesis, wound healing, DNA synthesis, and cell division [20]. ZHNs are unstable in low pH medium and when dissolved in lysosome (pH 4.5–5), zinc anions released and become part of the nutrient cycle [21]. In addition, Zinc compounds show interesting antibacterial properties [22]. In drug delivery systems, various drug carriers such as polymeric nanoparticles [23], dextran [24], and chitosan [25] have used NA.

In this work, we prepared an inorganic-organic drug carrier based on ZHN and chitosan host material intercalated with NA. The antibacterial and Controlled-release properties of the nanomaterial were investigated. In vitro release studies in buffer (pH 4.8 and 7.4) at 37 °C showed an initial burst effect followed by slow release. In addition, the antibacterial activity of the intercalation compound was evaluated against microorganisms. Fourier transform infrared (FTIR), Thermal analysis (TG/DTA), scanning electron microscope (SEM) and surface area studies on the composites are also discussed. The controlled release of NA from NA-ZHN and NA-ZHN/chitosan nanocomposite in buffer solution has been performed and monitored by UV–visible spectroscopy.

2. Experimental

Nalidixic acid was purchased from Alborz drug Company in Iran. All other reagents were purchased from Merck chemical company and used without further purification.

2.1 Synthesis

2.1.1 Synthesis of ZHN. ZHN was synthesized by dissolving 13.25 g (0.069 mol) of $Zn(NO_3)_2.6H_2O$ in 20 ml of distilled water, followed by precipitation by slow addition of 50 ml of aqueous 0.75 $molL^{-1}$ NaOH under magnetic stirring. The white precipitate obtained was collected by filtration and washed

three times with deionized water. The material was then dried at 50°C in a vacuum.

2.1.2 Synthesis of NA-ZHN. NA-ZHN was synthesized by method of anion exchange. As described elsewhere [18], NA solution was prepared by dissolving 0.1mol NA in 50 ml of water and then 0.2 g of the ZHN was added and stirred at room temperature for 30 min. Then, 0.1 $molL^{-1}$ NaOH solution was added drop wise with stirring until pH=8 was reached. The suspension formed was magnetically stirred for 24 hr. The solid was centrifuged and washed with decarbonated water three times and dried at 60 °C in a vacuum.

2.1.3 Synthesis of NA/chitosan and NA-ZHN/chitosan nanocomposite. Chitosan (0.15 g) was dissolved in 50 ml of 1% (v/v) acetic acid aqueous solution at 60 °C for 2hr. A suspension was prepared from 0.075 g of nalidixic acid or nalidixic acid-ZHN in 20 ml of deionized water. This suspension was added drop wise to the warmed suspension of chitosan. The pH was adjusted to 8 with 1 mol L^{-1} NaOH under the magnetic stirring at 60 °C for 24 hr. The white precipitate was filtered and washed three times with deionized water and dried at 60°C in a vacuum.

2.2 Characterization

The powder X-ray diffraction patterns (XRD) of the samples were collected with a Bruker AXS model D8 advance diffractometer using CuK_{α} source (λ=1.542 Å) at 40 KV, 35 mA, and a scan range 2°–70°. Infrared spectra were recorded with a Bruker Fourier transform infrared spectroscopy (FT-IR), using KBr pellets, scanned from 4000 to 400 cm^{-1}. Absorption spectra were recorded in the range 200-800 nm on a Shimadzu model 1601 PC UV-Visible spectrophotometer. The thermal behavior of the samples was determined by the thermogravimetric analysis (TGA) on a Mettler-Toledo TGA 851e

apparatus with a heating rate of 10 °C min^{-1} under the N_2 atmosphere. Scanning electron micrographs (SEMs), were taken on a KYKY-EM3200 and VEGA-TESCAN. The nitrogen adsorption–desorption isotherms of the samples were measured at 77 K using a micromeritics ASAP 2020 analyser. The specific surface area was obtained using the Brunauer-Emmett-Teller (BET) method and pore size distribution was evaluated using the Barrett–Joyner–Halenda (BJH) method.

2.3 Drug-release studies

The release of NA from ZHN, NA-ZHN/chitosan and plain NA was performed in a medium of PBS (phosphate buffered saline) at pH 7.4 and 4.8 at 37 °C. These solutions were stirred at 100 rpm on a magnetic stirrer for 24 hr. *In vitro* drug release studies were studied using a dialysis membrane. 0.01 g of the obtained NA or its nanocomposites was poured in a porous dialysis membrane. Every 10 min, 3 ml of the solution was removed and immediately replaced by an equal volume of fresh buffer solution (to keep the diffusion medium constant). The amount of drug released was monitored by a UV–Vis spectrophotometer at 257 nm.

The percent of the drug release was evaluated by using the following definitions:

$$\text{Drug Release (\%)} = \frac{\text{Amount of drug release (mg)}}{\text{Total weight of drug sample (mg)}} \times 100$$

2.4 Antimicrobial Activity

The antimicrobial activity of NA-ZHN and NA-ZHN/chitosan were evaluated against the following pathogenic strains: *S. Aureus* ATCC 25923, *B. subtilis* ATCC 1023 and *E. coli* ATCC 25922. Disk diffusion method was used to study the antimicrobial efficiency of prepared nanocomposites [27]. The antimicrobial activity was determined at a concentration of 20 μg ml^{-1} and their efficacy was

assessed on Muller Hinton agar disks. All the solutions were prepared in 0.1 mol L^{-1} NaOH. The bacterial cultures were grown overnight at 37 °C in a nutrient broth medium and then the suspension was diluted to 0.5 McFarland standard (10^6 CFU ml^{-1}). A lawn culture was made with these bacterial loads on Muller Hinton Agar plates. A filter paper disk (9mm) impregnated with 10 µL of nanocomposite was suspended in the sterile alkaline water and placed on the surface of the agar using a dispenser. The plates were inverted and incubated for 24 hr at 37 °C. The inhibition ring diameter of growth, which appeared around the disks, was measured. Gentamicin used in a concentration of 20 µg ml^{-1} as standard antibacterial.

2.5 Determination of the minimum inhibitory concentration (MIC)

The Minimum Inhibitory Concentration (MIC) assay is a technique used to determine the lowest concentration of a particular antibiotic needed to kill bacteria. MICs can be determined on plates of agar dilution or broth dilution methods. The MIC of the synthesized NA-ZHN and NA-ZHN/chitosan determined by microdilution broth method. The nanocomposite was tested at different concentrations of 10, 5, 1, 0.5, 0.1, 0 µg ml^{-1} in alkaline water. The MIC performed using 96-well plate with Muller Hinton broth medium with different concentrations of nanocomposite with standard antibiotic as positive and alkaline water as negative control. The 100 µl of Mueller Hinton Broth (10^6 CFU ml^{-1}) was added to the 100 µl aliquot of each dilution. The 96 well MIC plates were prepared in triplicate. The microbial cultures were incubated at 37 °C for 24 hr. The MIC was determined by comparing the various concentrations of nanocomposites showing different inhibitory effect.

3. Results and discussion

NA-ZHN nanocomposites were obtained using ion-exchange method of the ZHN on NA drug with the aim of improving biological properties. Microstructural characterizations of NA-ZHN nanocomposite was done by PXRD, FT-IR spectra, thermal gravimetric analyses, and BET analysis. The morphology of nanocomposites were studied by SEM. Antibacterial activity of nanocomposites were carried out using disk diffusion and minimum inhibitory concentration, and finally, the release of NA molecules from nanocomposite were studied in phosphate-buffered saline (PBS).

3.1 Microstructural analysis of the drug intercalated ZHN

PXRD patterns for NA, NA-ZHN and ZHN are given in Figure 2. The PXRD pattern of NA showed that the solid has good crystallinity. The PXRD pattern of ZHN confirms the formation of layered structure with the basal spacing of 9.57 Å. The sharp peak at $2\theta = 9.32$ is due to the 200 planes of the monoclinic lattice. The NA-ZHN composite obtained after anion exchange with NA, showed a peak at 8.22° in 2 θ, which corresponds to a basal spacing of 11.74 Å. This indicates successful intercalation of NA into the interlayers of ZHN as reflected by the observation of peak at lower 2θ value. When the ratio of the NA:ZHN was changed, there was no considerable difference the PXRD patterns of the resulting samples. Figure 3 shows the 3D molecular size of NA. Using MarvinSpace software, the long and short axes of NA were estimated to be 8.03 and 7.16 Å respectively (Figure 3A). After intercalation of NA, the interlayer distance is increased to 11.74 Å, with the thickness of the zinc hydroxide nitrate basal layer being 4.8 Å [28] and the gallery heights estimated to be 4.34 Å. The obtained value is smaller than the phenomena l length of NA molecule. This smaller d-spacing value suggests that the NA anions are arranged as a monolayer between the ZHN interlayers, with the carboxylate groups positioned towards the ZHN layers (Figure 3B). The possibility of the formation of

a zinc salt of NA cannot be excluded.

Figure 4 shows the infrared spectrum of the sample. Figure 4A shows the FTIR spectrum of pure NA. Strong bands at 1712 and 1617 cm^{-1} are characteristic of the stretching vibrations of carbonyl group of carboxylic acid and pyridone, respectively. Aromatic hydrocarbons show absorption in the region 1444 cm^{-1} due to C-C stretching vibrations in the aromatic ring. Nitrogen-Carbon-Hydrogen (NCH) deformation bands occur in the regions 1518, 1470, 1294-1050 and 705-776 cm^{-1}. The bands observed at 1370, 1479, 1518 cm^{-1} are assigned to C=N stretching vibration mode. Bonds at 2984 and 2945 cm^{-1} is assigned to aliphatic CH stretching vibration of ethyl and methyl group present in NA [29]. The FTIR spectrum of the ZHN is shown in Figure 4C. The peaks at 436 and 468 cm^{-1} are assigned to zinc-oxygen bond. The band observed at 641 cm^{-1} is due to the δ-mode of the O–H group O–H stretching. The sharp absorption at 1373 cm^{-1} and weak absorption at 833 cm^{-1} is due to N–O stretching, the latter being characteristic of D_3h (ν_3 mode).The 3486 cm^{-1} band may be due to the vibrations of the hydroxyl group which are hydrogen bonded to the nitrate groups in the interlayer. The sharp peak at 3580 cm^{-1}, due to stretching vibrations of hydroxyl groups belonging to the inorganic lattice. An absorption band at 1640 cm^{-1} is attributed to the bending mode of water molecules [30]. In the NA-ZHN nanocompsite (Figure 4B), the weak bands around at 3050 cm^{-1} due to =C-H are characteristic peak of aromatic compounds. Bands at 2980–2950 cm^{-1} are attributed to ethyl and methyl stretching. A broad band at 3336 cm^{-1} is attributed to the O-H stretching vibration of hydroxyl group. The stretching bands of asymmetric and symmetric of COO^- group of the NA anions can be observed at 1575 and 1388 cm^{-1}, respectively. In addition, the characteristic peak at 1260 cm^{-1}, is attributed to the stretching vibration of C–N group. The characteristic C=O stretching vibration of COO^- group at 1712 cm^{-1}has vanished in the NA-ZHN. This result indicates that NA in the NA-ZHN interlayer takes the form that has a negatively charged oxygen atom. The band at 762 cm^{-1} is due to hydroxyl bending

within the layers. Two bands at 444 and 495 cm^{-1} are due to the lattice vibrations of Zn–O and Zn-OH. These results further confirmed that NA has been intercalated into the interlay space of ZHN.

3.2 Thermal stability and surface morphologies of the hybrids.

The thermogravimetric and differential thermogravimetric analyses obtained for NA and NA-ZHN are shown in Figure 5. The TGA-DTG thermograms for NA show a single stage of weight loss at 316.2 °C, which can be due to combustion of the drug NA. For NA-ZHN, three steps of weight loss were observed (Figure 5B). The first step of weight loss is due to the removal of surface physisorbed water molecules at 43.5 °C. The second step of weight loss at 92.8 °C is attributed to the removal of interlayer anion and dehydroxylation of the OH layer. The last step of weight loss is due to decomposition of the intercalated anionic and dehydroxylation of the OH layer at 343.5°C. The decomposing temperature of the composite was slightly greater (343.51 °C) than that of the pristine NA drug (316.2 °C) indicates that NA-ZHN nanocomposite is thermally more stable than the unbound compound. This may be due to the encapsulation effect of drug inside the LDH gallery space.

Figure 6A and 6B shows the adsorption-desorption isotherms curve for NA-ZHN and ZHN. The shape of the isotherm curve for both materials shows Type IV behavior under IUPAC classification, indicating a mesopore type of material. For ZHN, the N_2 uptake was slow at the relative pressure in the range of 0.0–0.7, followed by rapid adsorption of the adsorbent at 0.7until an optimum adsorption of 65 cm^3g^{-1} was achieved. The isotherm for NA-ZHN adsorption increased from the relative pressure of 0.0 to 0.68 and reached peak at 90 cm^3g^{-1}. Then the adsorption increased slowly in the range 0.68-0.8, followed by the increase of the relative pressure range 0.8-1.0, and reached an optimum peak at 140 cm^3g^{-1}. For ZHN, the desorption branch of the hysteresis loop was narrower compared with NA-ZHN may be due to different pore texture.

The surface area of the drug and nanocomposite determined by the BET technique are shown in Table 1. The surface area for NA-ZHN 108.45 m^2g^{-1} increase compared to 22.56 m^2g^{-1} for ZHN is due to a change in the pore texture and formation of the nanocomposite lamellar. The BJH pore volume and the average pore diameter by BJH desorption is shown in Table 1. The average pore diameter increased from 5.76Å for ZHN to 20.17 Å for NA-ZHN due to the intercalation of NA into the ZHN. The BJH desorption pore volume increased from 0.089 cm^3g^{-1} to 0.203 cm^3g^{-1} for ZHN and NA-ZHN, respectively.

Figures 7A, 7B and 7C show the SEM images of ZHN,NA-ZHN and NA-ZHN/chitosan. In Figure 7A showed flake-like particles that are collected together with various sizes. This structure was transformed into a ribbon-like structure when the NA-ZHN nanocomposite was formed by a direct reaction of ZHN with NA under an aqueous environment (Figure 7B). This confirmed that the intercalation of NA into the interlayer of ZHN resulted in a change of the surface morphology from a flake-like structure to a ribbon-like structure with sizes in the nanometer range. The morphology of NA-ZHN/chitosan is found to be sheet-like, as can be seen from image (Figure7C).

3.3 Antibacterial activities of drug intercalated layered hydrids

Antibacterial activities of NA-ZHN and NA-ZHN/chitosan tested against microorganisms using disk diffusion assays. The study of disc diffusion indicated that NA-ZHN/chitosan and NA-ZHN composite are the most active nanocomposite with zone of inhibition of 49 mm E. coli and 37 mm against S. aureus composite. On the other hand, the uses of NA showed the lowest effect on all tested microorganisms in Table.2. The average size of the particle was around 200 micrometer for NA in the microparticles scale. The antibacterial ability of NA-ZHN might be referred to their small size, which is 100 times smaller than NA. The size of particles plays a significant role in antibacterial activity. The

antibacterial activity of NA-ZHN nanocomposite is influenced by the dimensions of the particles, smaller particles have a greater antimicrobial effect because the particles get smaller; their surface area to volume ratio increases and smaller particles have an easier time getting through the cell membrane and cell wall and that relative to larger nanoparticles [31].

Nanocomposites possess well-developed surface chemistry, chemical stability that make them easier to interact with the microorganisms and easier to adhere with the cell wall of the microorganisms causing its destruction and leads to the death of the cell [32,33].This could be explained based on the nature of the material present in cell wall. Gram-negative bacteria are surrounded by a thin peptidoglycan cell wall and Gram-positive are surrounded by layers of peptidoglycan many times thicker than is found in the Gram-negatives. Thus, an easier permeability could be achieved in the case of Gram-negative organisms. This confirms, nanocomposites show higher antibacterial activity with *E.Coli.*

3.4 Minimum Inhibitory Concentration (MIC)

The antimicrobial activities of nanocomposite against microorganisms were studied by quantitatively in terms of MIC. Five nanocomposite suspensions at concentrations of 20, 10, 5, 1, 0.5 μg ml^{-1} were tested and the results are given in Table 3. The MIC of nalidixic acid-ZHN/chitosan against E. coli; and S. aureus, were the best affect at the both strains. The antimicrobial activity of nanocomposite may be related the presence Zn^{2+} ion, chitosan and particles size. Zinc ions exhibit antimicrobial activity against various bacterial and fungal strains [34] and chitosan is a versatile material with proved antimicrobial activity [35].

3.5 Release behaviors of NA-ZHN and NA-ZHN/chitosan

To investigate the drug release behaviors of ZHN and ZHN/chitosan nanocomposite, the samples were individually dispersed in PBS at pH 7.4 and 4.8. Figure 8 shows the release behaviors of chitosan, ZHN and ZHN/chitosan at pH 7.4 and 4.8. Figure 8A shows the effect of pH on the release performance of NA anions from the chitosan nanocomposite. At pH 7.4, the release rates of NA are slower than that at pH 4.8 and, the release percentage of NA from chitosan at pH 7.4 was about 72% at 540 min, compared to 85% at 390 min at pH 4.8.

The release rate of NA from ZHN and ZHN/chitosan is shown in Figure 8B and 8C. Figure 8B shows that the release of NA from ZHN was completed in 150 min at pH 4.8, compared with the slower release rate of NA at pH 7.4, where the time taken for 79% to be released was 150 min. This phenomenon is due to the electrostatic attraction between NA anions and the ZHN layers together with the ion-exchange property. These results confirmed the suitability of the ZHN intercalated systems for controlled release of the antibiotic drugs. ZHN is stable in a pH range of 7.4.The release behavior of NA shows a fast release at the beginning, 67% for the first 120 min, which is possibly due to very low dissolution of the ZHN because it is not stable in acidic media. The slow release process has been shown, may be related to the ion-exchange reaction between NA anion into the ZHN and phosphate anions in the buffer solution [36,37].

The percentage release rate NA-ZHN from chitosan at pH 7.4 reaches about 62% within about 640 min, compared to about 70% within about 450 min at pH 4.8. The NA-ZHN nanocomposite shows a faster release rate than NA-chitosan, while, NA-ZHN/chitosan nanocomposite shows slower release rate than NA-chitosan and NA-ZHN. Therefore, this result confirms that the NA-ZHN and NA-ZHN/chitosan nanocomposites show a good potential to be used for controlled release drug delivery.

4. Conclusion

Nalidixic acid-Zinc Hydroxide Nitrate nanocomposite was synthesized by intercalating Nalidixic acid into the interlayer space of Zinc Hydroxide Nitrate by ion- exchange method. Then, Nalidixic acid-Zinc Hydroxide Nitrate/chitosan nanocomposite has been prepared. To prove that interlayer nitrate ions were replaced by Nalidixic acid anions was used to X-ray diffraction, Fourier Transform Infrared, and thermogravimetric analysis. The Nalidixic acid-Zinc Hydroxide Nitrate showed a gallery height of 4.34 Å and Nalidixic acid anions were arranged with the tilting angle of 32 in the interlayer with monolayer arrangement. FT-IR spectroscopy exhibits the presence of functional groups of both Zinc Hydroxide Nitrate layers and Nalidixic acid anions. Antibacterial activity of the nanocomposite studied by the diffusion disc method and theses result showed that antibacterial activity of nanocomposite more than the drug Nalidixic acid. *In vitro* drug release the Nalidixic acid-Zinc Hydroxide Nitrate and Nalidixic acid-Zinc Hydroxide Nitrate /chitosan show that the release rate Nalidixic acid-Zinc Hydroxide Nitrate /chitosan nanocomposite is remarkably lower than that from the Nalidixic acid chitosan and Nalidixic acid-Zinc Hydroxide Nitrate /chitosan at pH 7.4. All of these results suggest that Nalidixic acid-Zinc Hydroxide Nitrate and Nalidixic acid-Zinc Hydroxide Nitrate /chitosan materials are suitable for drug delivery and biological application.

Acknowledgments

Financial support from Azarbaijan Shahid Madani University research council is greatly appreciated.

References

[1]. M. Z. Hussein, N. Hashim, A. Hj. Yahaya, Z. Zainal. Solid State Sci.12 (2010) 770–775.

[2]. S. H. Al Ali, M. Al-Qubaisi, M. Z. Hussein, M. Ismail, Z. Zainal, and M. N. Hakim. Int J Nanomed.7 (2012) 3351–3363

[3]. M. Ogawa, K. Kuroda. Chem. Rev. 95 (1995) 399–438.

[4]. P. Laurence, J. Noureddine, F. Fernand. Chem.Mater.12 (2000) 3123.

[5]. G. R. William, D. O'Hare, J. Mater.Chem.16 (2006) 3065.

[6]. M. Z. Hussein, S. H. Sarijo, A. Yahaya, Z. Zainal, J. Nanosci. Nanotechnol.7 (2007) 2852-62.

[7]. E. Kandare, J. M. Hossenlopp, J. Phys. Chem.B 109 (2005) 8469.

[8]. L. Tammaro, U. Costantino, A. Bolognese, G. Sammartino, G. Marenzi, A. Calignano, S. Tete´ , F. Mastrangelo, L. Califano, V. Vittoria, Int. J. Antimicrob. Ag. 29 (2007) 417.

[9]. M. R. Berbera, K. Minagawaa, M. Katoha, T. Morib, M. Tanaka, Eur. J. Pharm. Sci. 35 (2008) 354.

[10]. Q. H. Zeng, A. B. Yu, G.Q. Lu, D. R. Paul, J. Nanosci.Nanotechnol.5 (2005) 1574.

[11]. R. Marangoni, L. P. Ramos, F. Wypych, J. Colloid Interface Sci. 330 (2009) 303.

[12]. F. Barahuie, M. Z.r Hussein, S. Fakurazi , Z. Zainal, Int. J. Mol. Sci.15 (2014) 7750-7786.

[13]. M. Louer, D. Louer, D. Grandjean. ActaCrystallogr B. 29 (1973) 1696–1703.

[14]. W. Stahlin, H. R. Oswald. ActaCrystallogr B. 26 (1970) 860–863.

[15]. M. Z. Hussein, Ali. SH. Al, Z. Zainal, M.N. Hakim. Int J Nanomedicine 6 (2011) 1373-1383.

[16]. S. Hasan, Ali.H. Al, M. Al-Qubaisi. Int J Nanomedicine. 7 (2012) 3351.

[17]. F. Barahuie, M. Z. Hussein, Sh. AbdGani, Sh. Fakurazi, Z. Zainal. Int.J.Nanomedicine. 9 (2014) 3137–3149.

[18]. P M. de la Torre, Y. Enobakhare, G. Torrado, S. Torrado. Biomaterials. 24 (2003) 1499-506.

[19]. M. Trikeriotis and D. F. Ghanotakis, Int. J. Pharmaceutics 332 (2007) 176–184.

[20]. K. Jeejeebhoy, Gastroenterology. 137 (2009) S7–S12.

[21].S. J. Xia, Z. M.Ni, Q. Xu, B. X. Hu, J. Hu. J Solid State Chem. 181(10) (2008) 2610–2619.

[22]. U. Faiz, T. Butt, L. Satti, W. Hussain, F. Hanif. J Ayub Med Coll Abbottabad. 23(2) (2011) 18–21.

[23]. A. Abouzarzadeh, M. Forouzani, M. Jahanshahi, N. Bahramifar , J Mol Recognit. 25(7) (2012) 404-13.

[24]. J. S. Lee , Y. J. Jung , M. J. Doh and Y. M. Kim. Drug Dev Ind Pharm. 27(4) (2001) 331-6.

[25]. M. Georgeta, A.-JaudetElie, L. Didier, P. Luc, C. Adrian and M. Guy. Current Drug Delivery. 1(3) (2004) 227-33.

[26]. J. Berger, M. Reist, J. M. Mayer, O. Felt, and R. Gurny, Eur. J. Pharm. Biopharm, 57 (2004) 35.

[27]. C. Perez, M. Pauli, P. Bazevque, Acta Biologiae Et. Medicine Experimentalis, (1990) 113-115.

[28]. C. Misra, A. J. Perrota. Clays Clay Miner. 40 (1992) 145–150.

[29]. A. Debnath, N.K. Mogha, D.T. Masram. Appl Biochem Biotechnol. 175 (5) (2015) 2659-2667.

[30]. W. Stählin, H. R. Oswald, Acta Crystallogr., Sect. B: Struct. Sci. 26 (1970) 860.

[31]. Nirmala G A and Pandian K. Journal of Colloids and Surfaces A: Physicochem. Eng. Aspects.297 (2007) 63–70.

[32]. G. Rezaie Behbahani, M. Hossaini Sadr, H. Nabipour, Biophys. Rev. Lett. 08 (2013) 51.

[33]. B. D. Korant, J. C. Kauer, B. F. Butterworth, Nature, 248 (1974) 588.

[34]. E. De Clercq. Metal-Based Drugs, 4 (1997) 173.

[35]. R. C. Goy, D.de Britto, Odilio B. G. Assis, Polímeros: Ciência e Tecnologia, 19 (3) (2009) 241-247.

[36]. V. Ambrogi, G. Fardella, G. Grandolini, L. Perioli, MC. Tiralti.AAPS Pharm Sci Tech. 3 (2002) 77–82.

[37]. M. Z. Bin Hussein, Z. Zainal, A. H. Yahaya, and D. W. V. J. Control Release.82 (2002) 417–427.

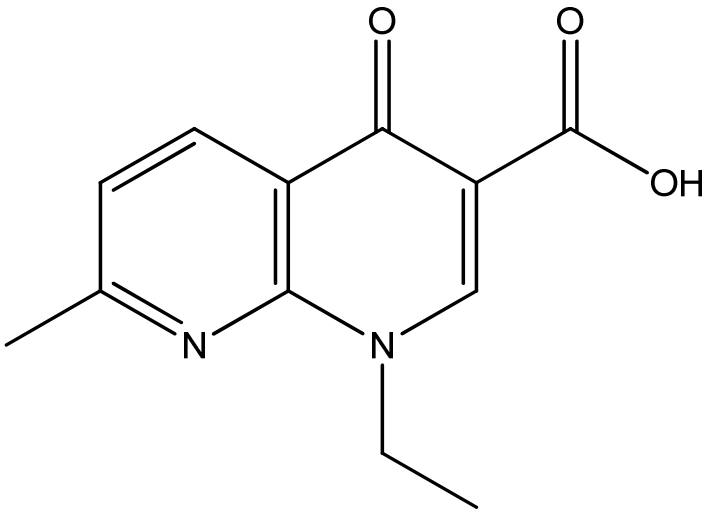

Figure 1.Chemical structure of Nalidixic acid.

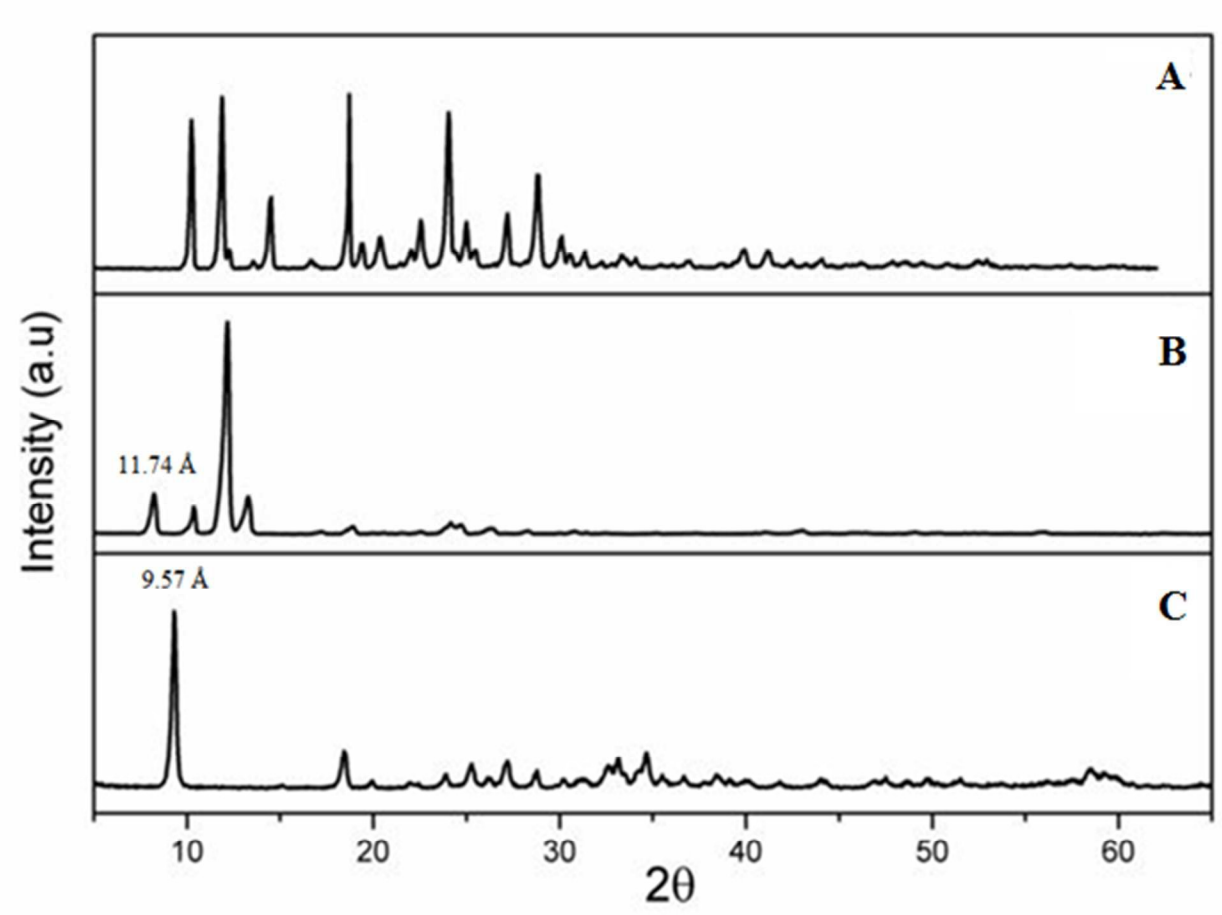

Figure 2. Powder X-ray diffraction patterns of A) Nalidixic acid, B) Nalidixic acid-ZHN, C) ZHN

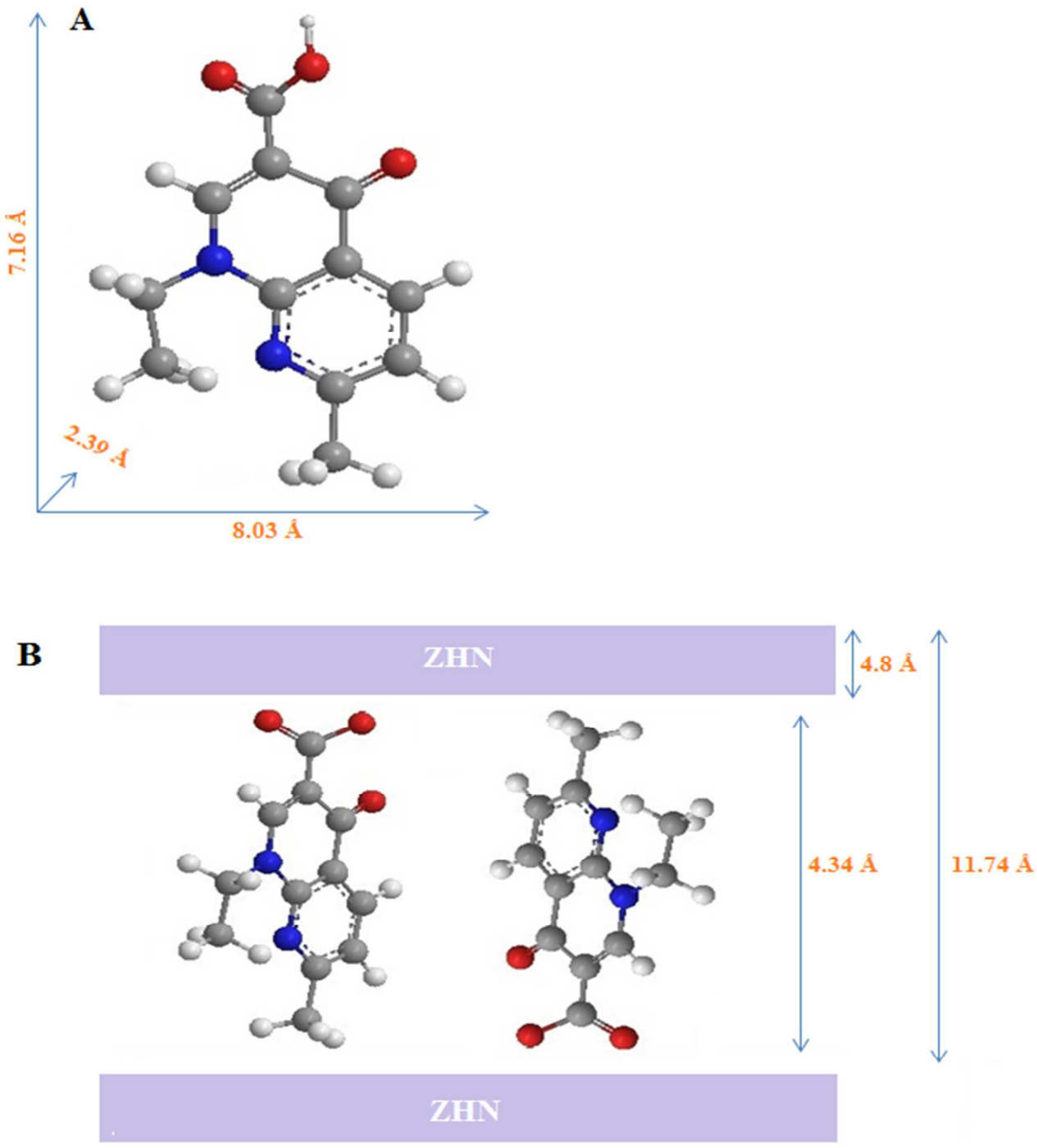

Figure 3. A) Molecular dimensions of Nalidixic acid molecule. B) Schematic arrangement of Nalidixic acid anions in the interlayer space of Nalidixic acid-ZHN.

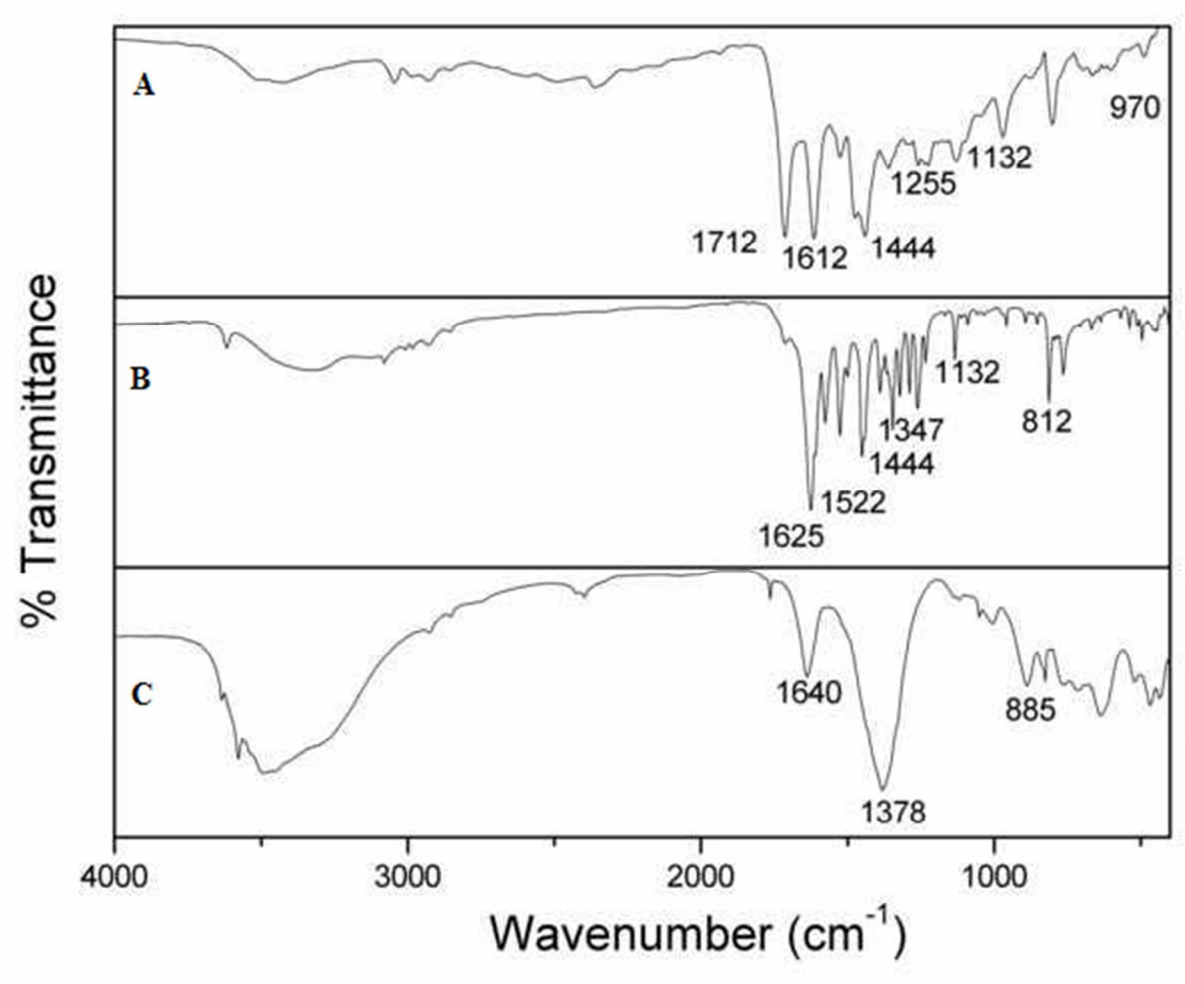

Figure 4. FTIR spectra of A) Nalidixic acid, B) Nalidixic acid-ZHN, C) ZHN

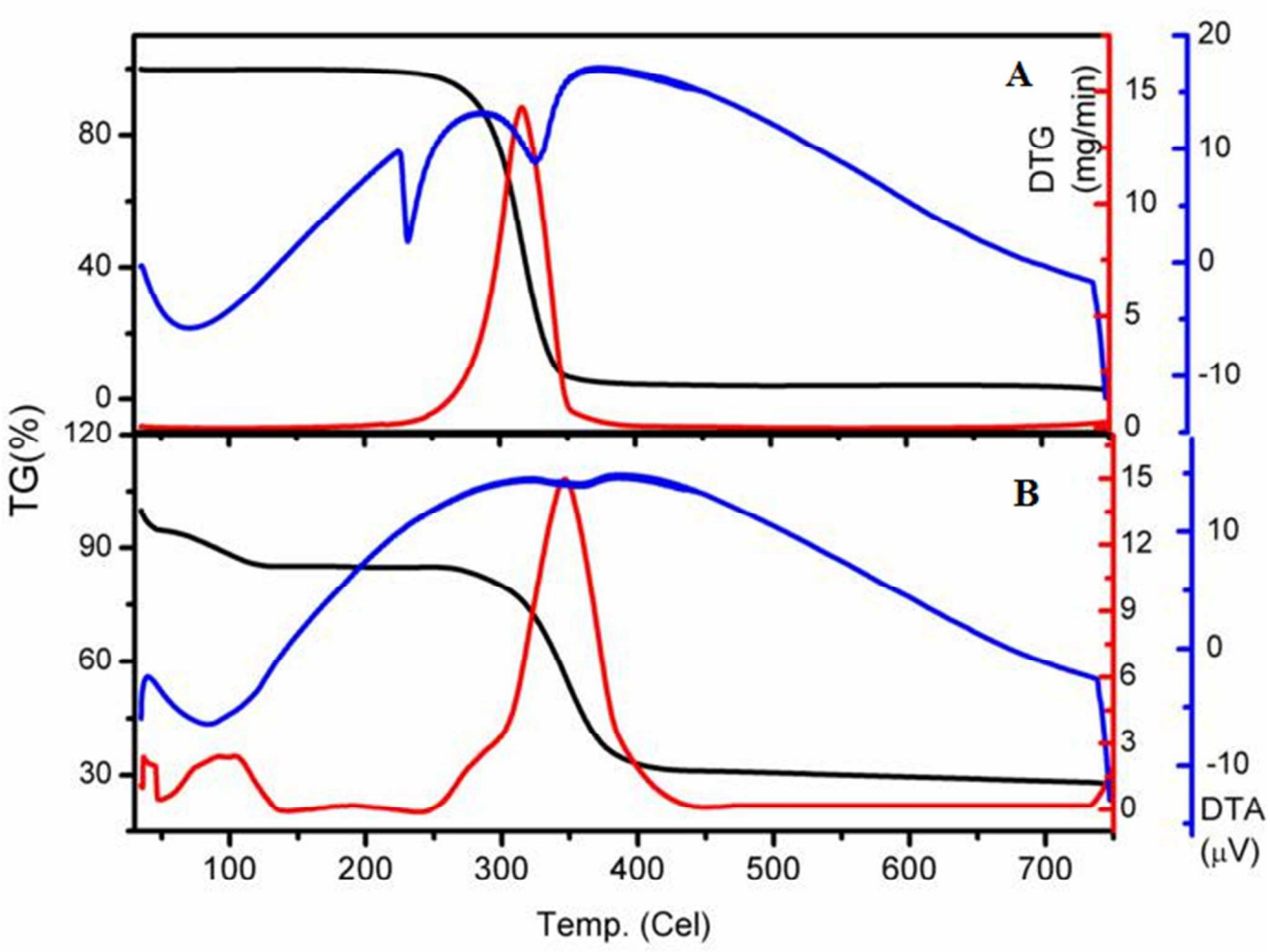

Figure 5. TGA-DTG thermograms of A) Nalidixic acid, B) Nalidixic acid-ZHN

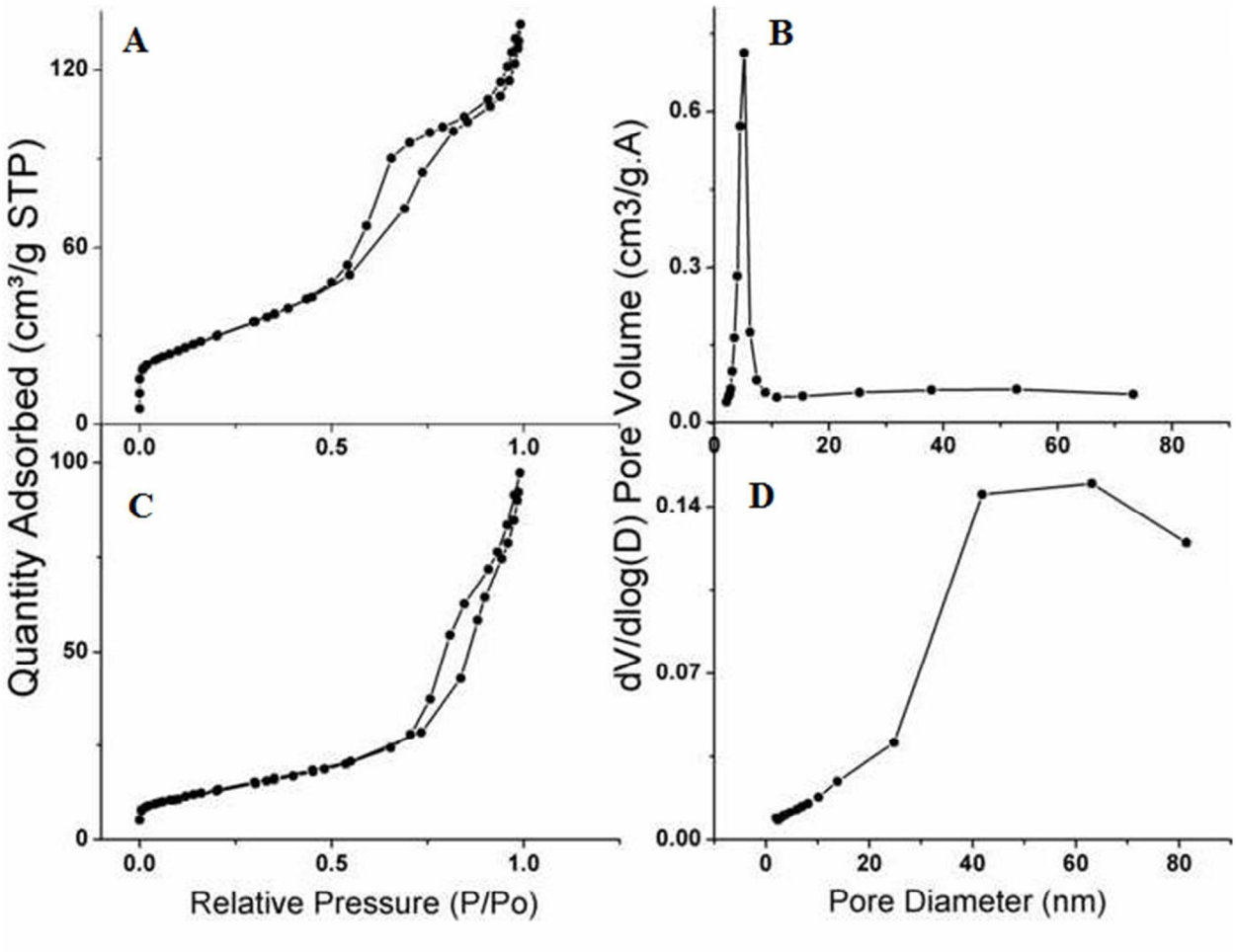

Figure 6. Nitrogen adsorption–desorption isotherms of A) Nalidixic acid-ZHN and B) ZHN, and BJH pore size distribution of C) Nalidixic acid-ZHN and D) ZHN.

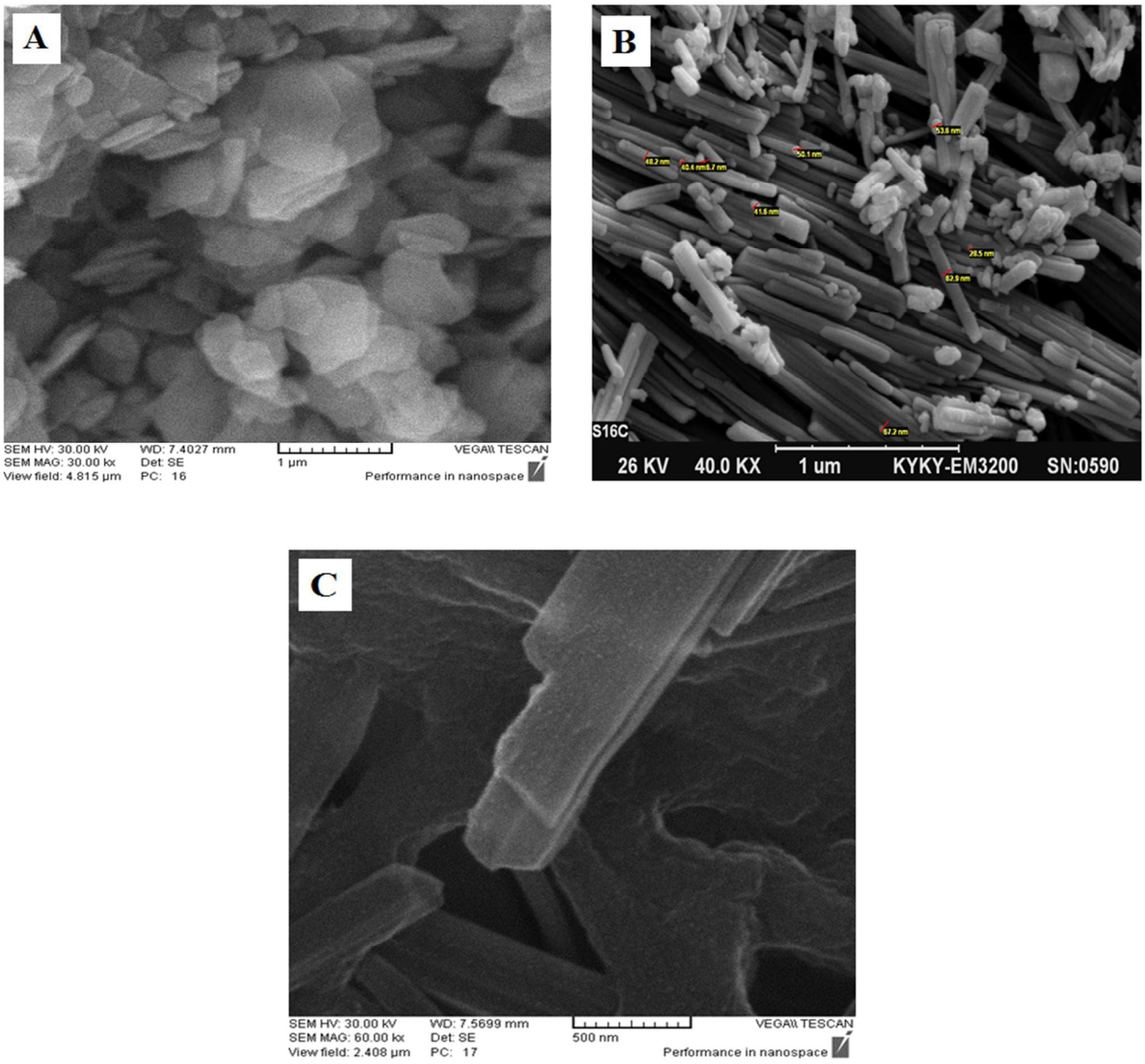

Figure7. SEM images of A) ZHN, B) Nalidixic acid-ZHN C) Nalidixic acid-ZHN/Chitosan

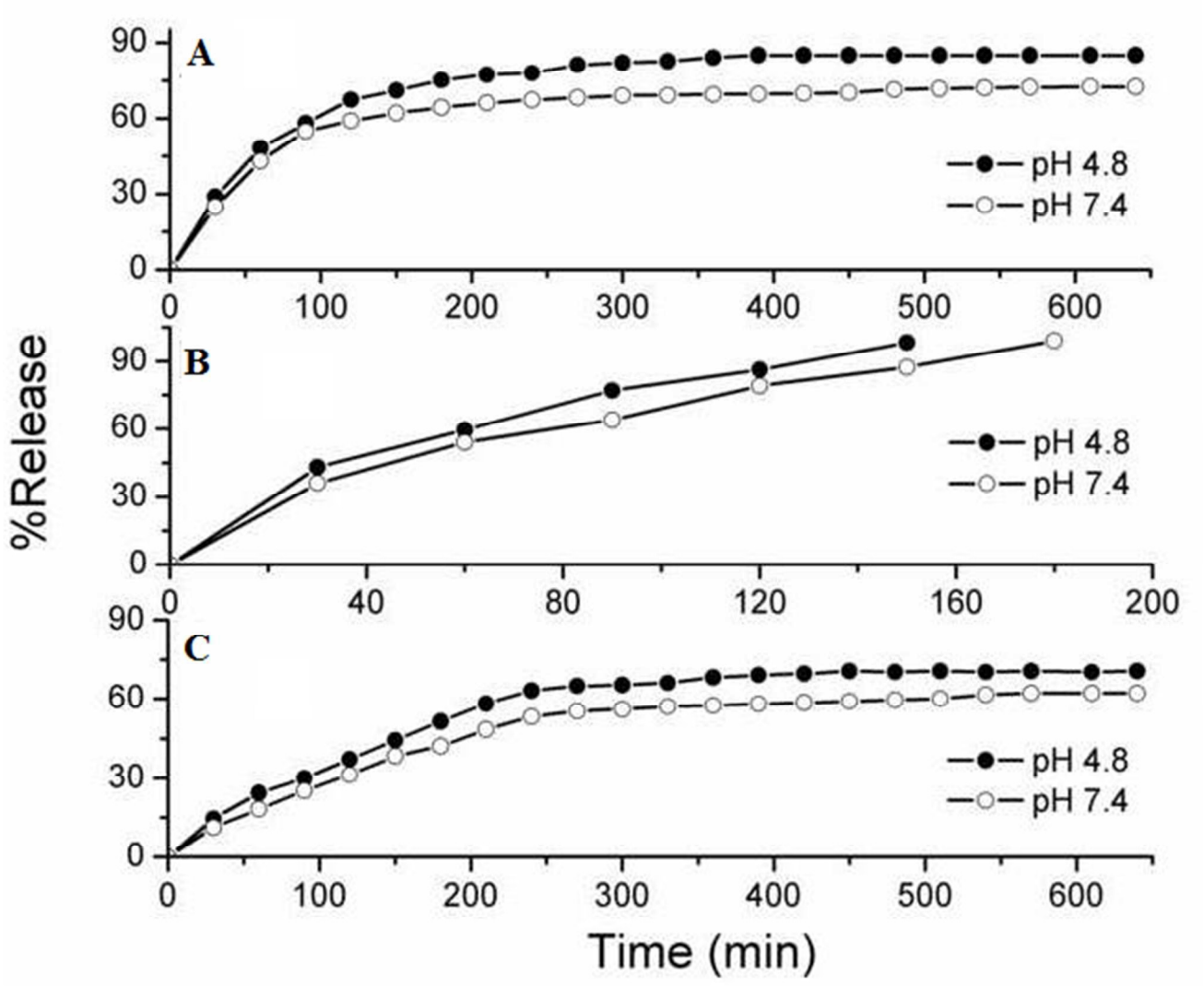

Figure 8. Release properties of Nalidixic acid from A) Chitosan, B) ZHN, C) ZHN-Chitosan nanocomposite at pH 4.8 and pH 7.4.

Table 1. Textural properties of ZHN and Nalidixic acid-ZHN

Sample	BET surface area (m^2g^{-1})	BJH pore volume (cm^3g^{-1})	BJH average pore diameter(nm)
ZHN	22.56	0.089	5.76
Nalidixic acid-ZHN	108.45	0.203	20.17

Table 2. Antibacterial activities of Nalidixic acid, Nalidixic acid-ZHN and Nalidixic acid-ZHN/Chitosan against pathogenic microorganisms.

Bacterium	**Zone of Inhabitation (mm)**		
	Nalidixic acid	Nalidixic acid-ZHN	Nalidixic acid-ZHN/Chitosan
S. aureus	<13	29	37
B. subtilis	<13	24	34
E. coli	19	33	49

Table 3. Antibacterial activities (MIC values in μg ml^{-1}) Nalidixic acid-ZHN and Nalidixic acid-ZHN/Chitosan against pathogenic microorganisms.

Bacterium	**MIC (μgml^{-1})**		
	Nalidixic acid	Nalidixic acid-ZHN	Nalidixic acid-ZHN/Chitosan
S. aureus	>5	>1	>1
B. subtilis	>10	>5	>5
E. coli	>1	>0.5	>0.5

Graphical Abstract

Nalidixic acid intercalated Zinc Hydroxide Nitrate is suitable for a controlled-release formulation and nanocomposite is an effective antibacterial agent.